Journal of the European Ceramic Society **11** (1993) 299–308

High-quartz Solid-solution Phases from Xerogels with Composition $2MgO.2Al_2O_3.5SiO_2$ (μ-Cordierite) and $Li_2O.Al_2O_3.nSiO_2$ ($n = 2$ to 4) (β-Eucryptite): Characterization by XRD, FTIR and Surface Measurements

D. Mazza,[a] M. Lucco-Borlera,[a] G. Busca[b] & A. Delmastro[a]

[a] Dipartimento di Scienza dei Materiali e Ingegneria Chimica, Politecnico, Torino, Italy
[b] Istituto di Chimica, Facoltà di Ingegneria dell'Università, Genova, Italy

(Received 28 July 1992; revised version received 21 September 1992; accepted 28 September 1992)

Abstract

The title phases are prepared by the sol–gel route employing prehydrolyzed tetraethylorthosilicate (TEOS) and Al, Li or Mg nitrates in aqueous solution. Amorphous xerogels are obtained at 400°C; they are characterized as high to very high surface oxides with peculiar pore-size distributions. High-quartz solid-solution phases originate from these xerogels by heating at 600°C (lithia-containing compositions) or at 900°C (magnesia-containing composition). They are characterized by X-ray powder diffraction and FTIR spectroscopy as phases with strong disorder in the cation distribution, both in the Al/Si sites and Li sites, with the exception of the stoichiometry $LiAlSiO_4$, which shows a certain degree of Li and Si/Al ordering.

Die untersuchten Phasen wurden über ein Sol–Gel-Verfahren aus teilhydrolysiertem Tetraethoxysilan (TEOS) und wässrigen Al-, Li-, oder Mg-Nitratlösungen hergestellt. Bei einer Temperatur von 400°C wurden amorphe Precursor erhalten, die sich als Oxide mit großer bis sehr großer Oberfläche und einer ungewöhnlichen Porengrößenverteilung herausstellten. Mischkristalle mit Hochquartzstruktur entstanden durch Erhitzen der Precursor auf 600°C bei LiO_2-haltigen Zusammensetzungen bzw. auf 900°C bei MgO-haltigen Zusammensetzungen. Die Mischkristalle wurden durch Röntgenbeugung und FTIR-Spektroskopie charakterisiert. Sie zeigten eine starke Fehlordnung in der Kationenverteilung, sowohl Al/Si- als auch Li-Plätze betreffend. Eine Ausnahme bildete die Verbindung $LiAlSiO_4$, die einen gewissen Ordnungsgrad für Li und Si/Al zeigt.

Les phases object de la recherche ont été obtenues par la méthode sol–gel en employant du tétraéthylorthosilicate (TEOS) précédemment hydrolisé, auquel on ajoutait les solutions acqueuses des nitrates d'aluminium, lithium et magnésium. A 400°C on obtient des solides amorphes: il s'agit de phases oxides avec une très grande surface et une particulière distribution des pores. Les phases contenantes du lithium chauffées à 600°C et celles contenantes du magnésium chauffées à 900°C donnent origine à des solutions solides ayantes la structure du quartz de haute température. Examinées par diffraction de rayons X et par spéctroscopie FTIR elles montrent une distribution très désordonnée des cations, soit dans les sites Al/Si, soit dans les sites Li. Il fait exception le solide de composition $LiAlSiO_4$ auquel correspond un certain dégré d'ordre soit pour le lithium, soit pour Al/Si.

1 Introduction

The so-called 'stuffed' β (high)-quartz structures[1] are known to exhibit interesting physical and technological properties. This name was given to structures in which the mode of linking of the tetrahedra in the quartz structure is retained, but some Si atoms are replaced by Al while cations (e.g. Li^+, Mg^{++}) are accommodated in some of the interstices to maintain charge balance[2] (Fig. 1(a)).

In the system Li_2O–Al_2O_3–SiO_2, β-quartz solid-solution phases of this type have found application for low-expansion glass ceramics.[3] The high-temperature structure of β-eucryptite ($LiAlSiO_4$) can be thought as a superstructure on β-quartz[4] with

Journal of the European Ceramic Society 0955-2219/93/$6.00

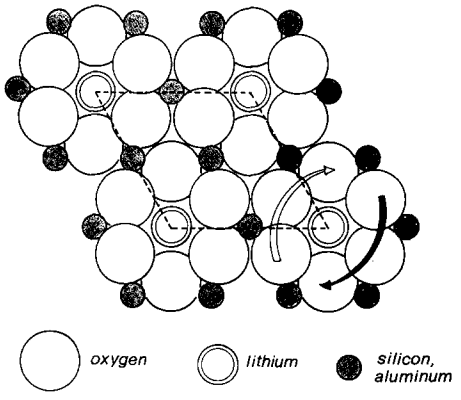

(a)

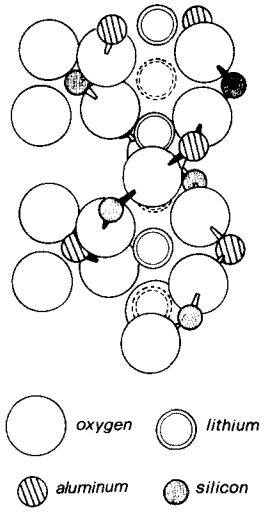

(b)

Fig. 1. Structure of β-eucryptite (a) viewed along the z edge, (b) projection onto the xy base plane.

half the silicon atoms replaced by aluminium, whereas lithium lies in some of the tetrahedral voids of the structure, located along the z edges of the unit cell (Fig. 1). Between β-eucryptite and SiO_2, β-quartz phase forms from the crystallization of glasses for nearly the whole compositional range.[5] For high SiO_2 contents, however, such phases are only metastable precursors of the stable equilibrium phase (β-spodumene solid solution).[6] This is confirmed by the study on the phase diagram of the system Li_2O–Al_2O_3–SiO_2 reported by Ref. 7, in which the stability field of β-eucryptite solid solution is confined to the range of compositions 1:1:1 to about 1:1:1·60 (Li:Al:Si).

In the system MgO–Al_2O_3–SiO_2 stuffed β-quartz structures are known to form only as metastable phase (μ-cordierite) that evolve by further heating into the stable modification α-cordierite.[8]

In this work the title phases with the stuffed β-quartz structure are prepared by an unconventional sol–gel technique, by means of the preliminary formation of an amorphous solid (xerogel). The preparative route employs pre-hydrolyzed silicon alkoxide and metal nitrates to try to overcome some of the problems encountered in the multicomponent alkoxide method. Indeed, a drawback of the latter method is the difficulty in preparing homogeneous precursor xerogels of silicates from alkoxides, as the difference in hydrolysis rate between silicon and other alkoxides causes preferential hydrolysis and hence the occurrence of micro- or nano-heterogeneities in the xerogels and in the related crystallization products.[9,10]

2 Experimental

2.1 Preparation

A measured volume of tetraethylorthosilicate (TEOS) is added to an equal volume of ethanol (95%) and half a volume of distilled water. The pH of the aqueous alcoholic phase is adjusted to 0·5–1·0 with a few drops of 1M HNO_3. In this way a clear solution is quickly obtained after a few minutes of stirring at room temperature. The r factor (water moles/TEOS moles) reaches a value of about 7.

Under these conditions TEOS is firstly partially hydrolyzed to silanol[11] monomers. An aqueous solution of aluminium and magnesium or lithium nitrates in proper amounts is then added to the stoichiometric quantity of the TEOS solution. The clear solution thus obtained is then treated with excess aqueous ammonia (10 wt%). Condensation and crosslinking of these silanols and gelation of the solution occurs, whilst the aluminium and magnesium hydroxides precipitate. The basic (pH = 10) gel obtained is first dried at 105°C and then gradually heated up to 400°C, thus removing excess water and gaseous products formed by the decomposition of nitrates, leaving a white crispy oxide powder.

The solids obtained by this procedure are found to be amorphous when examined by X-ray diffraction. The samples prepared were characterized by the following compositions (with respect to the unit cell of the β-quartz):

C1: $Mg_{0.67}Al_{1.33}Si_{1.67}O_6$
E1: $Li_{1.5}Al_{1.5}Si_{1.5}O_6$
E2: $Li_{1.33}Al_{1.33}Si_{1.67}O_6$
E3: $Li_{1.15}Al_{1.15}Si_{1.85}O_6$
E4: $Li_1Al_1Si_2O_6$

2.2 Differential thermal characterization

The xerogels obtained at 400°C were submitted to DTA in Netzsch 414 differential calorimeter with a heating rate of 10°C/min using Pt crucibles and about 50 mg of powder. The DTA curves (Fig. 2) are all characterized by two marked endotherms, the first beginning at about 200°C and the second

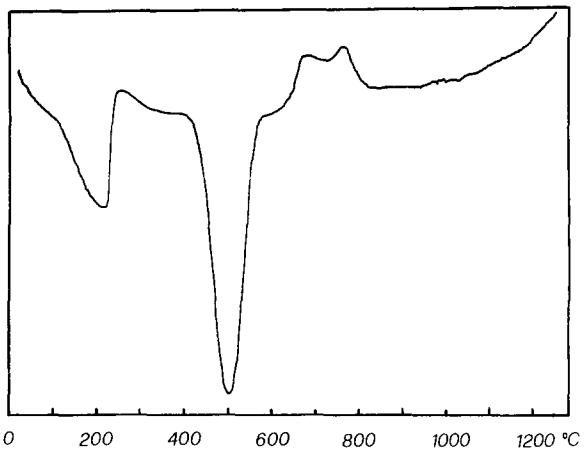

Fig. 2. Differential thermoanalysis (DTA) curve for amorphous E1 sample.

beginning at about 400°C with a maximum at 500°C (see Fig. 2 for example). Both of these are accompanied by a simultaneous weight loss, as shown by the thermogravimetry (curves not shown), and are due, in the authors' opinion, to the loss of the physically and chemically adsorbed water (first peak) and to the loss of surface hydroxyls with simultaneous decrease in surface area (second peak).

In a higher temperature range (600–700°C for lithia-containing compositions, 900–1000°C for magnesia) an exothermic peak occurs, due to the crystallization of the amorphous xerogel mass.

The XRD analysis performed on samples heat treated at temperatures preceding and following these exotherms allowed their assignment to a crystallization process. The same XRD analysis allowed the crystallization products to be characterized structurally.

2.3 BET characterization

The amorphous xerogels, as obtained at 400°C, are treated under dynamic vacuum at 105°C in order to eliminate adsorbed water from the surface.

Surface areas are determined through the BET adsorption (isotherms of N_2 at 77 K obtained with Carlo Erba Sorptomatic 1800). The pore distribution curves were obtained from the N_2 adsorption isotherm by means of the standard model of Hasley as reported by Lowell *et al.*[12] In Table 1 the surface areas of the different amorphous samples are

Table 1. Surface areas of the prepared samples

Sample	*Temperature (°C)*	*Time (min)*	*Area (BET) (m^2/g)*
E1	400	120	191
E2	400	120	222
E3	400	120	229
E4	400	120	198
C1	400	120	914, 810
C1	400 + 600	120 + 30	776
C1	400 + 800	120 + 30	641

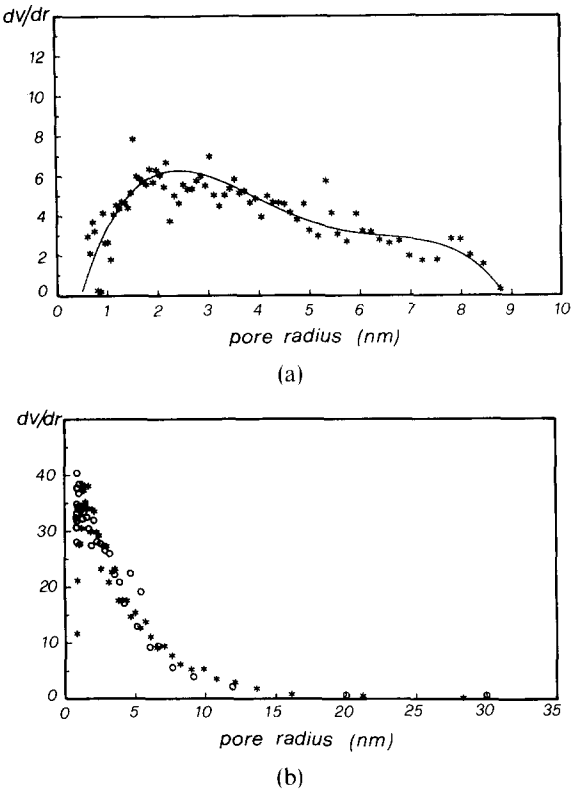

Fig. 3. (a) Pore-size distribution of an amorphous E1 sample; (b) Pore-size distribution of an amorphous C1 sample; *, adsorption; ○, desorption.

reported, and in Fig. 3 two characteristic pore distribution curves are shown.

The surface areas of the amorphous xerogels E1 to E4 are all characterized by values of 190 to 220 m^2/g and by a pore distribution curve, based on the data of the adsorption isotherm, with a very broad maximum around 3 nm (Fig. 3(a)).

The surface area of the amorphous xerogel C1 shows the very high value of 914 m^2/g: repeated BET measurement on a different sample prepared under the same conditions furnished the value of 810 m^2/g, indicating a fairly good repetition of its surface characteristics. Moreover, the pore distribution curves obtained in this case show a narrow maximum around 2 nm radius (Fig. 3(b)), with an exponential decrement for higher pore radii, a fact that could arouse interest for the use of this material as a support for porous inorganic catalysts. In this case both the adsorption and desorption isotherms were evaluated, yielding substantially coincident values.

The distribution curve remains unchanged in shape for heat treated xerogels at 600 and 800°C for 0·5 h, but the surface area lowers to 776 and 614 m^2/g respectively. At these temperatures the samples retain their amorphous state, whilst at temperatures higher than 900°C the μ-cordierite phase begins to crystallize. When this process is completed, the surface area is reduced to 18 m^2/g.

Some other chemical and physical characteristics

of the surface of these solids are under examination; they will be the subject of a further paper.

2.4 X-Ray diffraction

X-ray powder diffraction (XRD) analysis was performed with computer-aided Philips PW 1710 equipment (CuK_α radiation, graphite monochromator).

The XRD analysis was carried out at room temperature on samples obtained from amorphous xerogels, directly heat treated in air at the indicated temperatures for 30 min, unless stated otherwise.

All the samples obtained at 400°C show XRD patterns typical of amorphous phases (Fig. 4(a)), while they all show the formation of crystalline structures at temperatures higher than the DTA crystallization peak. For the samples E1 and E2 heated at 800°C, peaks of the low-temperature α-eucryptite structure are still evident, together with those of the high-temperature β-eucryptite (Fig. 4(b)): the former is most probably the first phase to crystallize from the xerogel; the peaks of the α-phase are still present for samples heated at 1000°C and disappear completely only at 1200°C, leaving the clean pattern of the β-eucryptite structure (β-quartz type) (Fig. 4(c)).

The samples E3 and E4 show at 800°C only the XRD peaks of the β-quartz solid solution while at 1000°C the peaks of the β-spodumene solid solution are already evident and finally at 1200°C this latter phase becomes the only one present. For these two last compositions it is thought that the β-quartz structure forms as the first crystallization product, but only as in a metastable phase, which evolves at higher temperature toward the stable equilibrium phase.

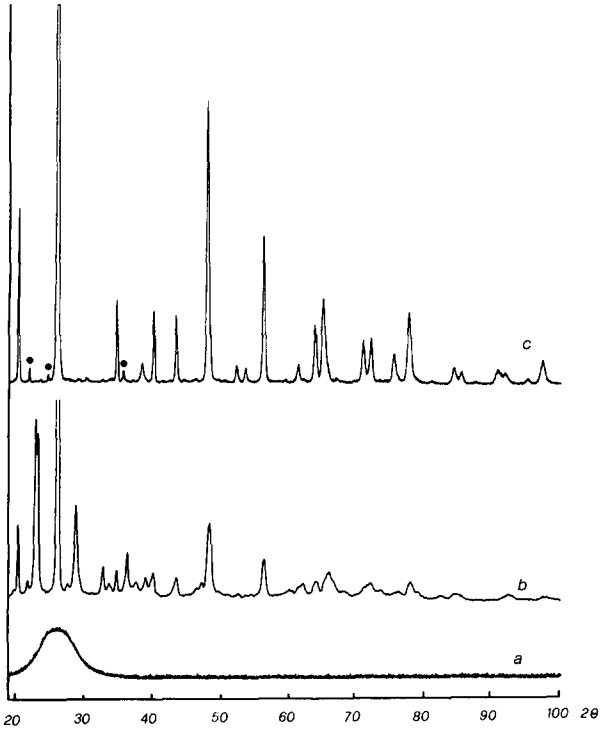

Fig. 4. X-Ray powder patterns of E1 (a) amorphous, (b) heated at 800°C and (c) heated at 1200°C (● = superstructure reflections).

The samples E1 and E2 heated at 1200°C and E3 and E4 heated at 800°C and constituted only by the pure β-quartz solid solution, were further characterized by XRD and FTIR. Only the sample E1 shows small but noticeable additional diffraction peaks which require a doubling of the c_0 cell parameter. However, no hint for doubling of the a_0 cell parameter is found on the XRD pattern. The samples E2, E3 and E4 do not display, under the conditions of preparation adopted, any XRD peaks indicative of a different unit cell from that of β-quartz solid solution.

This fact might be explained, in the authors' opinion, by the occurrence of only some of the ordering phenomena of β-eucryptite, as proposed by Pillars & Peacor.[13] In their single-crystal structure determination at different temperatures, these authors pointed out that for the stoichiometric composition (Li:Al:Si = 1:1:1), mutual ordering of Al and Si in the structural network and of Li in the tetrahedral voids of the structure exists at room temperature and in single crystals 'as grown' from flux. Indeed, they indexed the unit cell with both doubled a_0 (1·0497 nm) and c_0 (1·1200 nm) with respect to the β-quartz substructure. However, these authors found clear XRD evidence for a second-order transition, completing at about 460°C, which was allotted to a different ordering scheme of Li in the framework channels. XRD measurements at high temperature indicate, according to the same authors, that half of the lithium atoms are interchanging with the initially vacant sites as temperature increases. Indeed, lithium atoms occupy only half of the available sites in the channels, and the barriers to diffusion between sites should be low. Above the 460°C transition, the four low-temperature subcells related by the $a/2$ translation become translation-equivalent and therefore the a_0 is halved to the value of β-quartz, whilst c_0 remains unchanged. The same authors showed, in the samples examined, a limited Si–Al ordering in the tetrahedral framework, independent of the temperature, whilst Tscherry & Leaves[14] reported a complete Al and Si ordering over all sites of the same structure at room temperature. The difference in these results is probably a measure of the differences in synthesis conditions for the crystals which were investigated; evidently the Si–Al ordering depends essentially upon the preparative conditions of the samples.

A complete disorder between Al and Si atoms would render all the tetrahedral inter-channel positions equivalent and hence imply an

Table 2. Structural parameters for the E1 sample (1200° C)

Position	x/a_0	y/b_0	z/c_0	*Occupancy (%)*	*Thermal factor*
Si in 3*c*	0·5	0	0	100	0·5
Al in 3*d*	0·5	0	0·5	100	0·5
Li in 3*a*	0	0	0	31 ± 8	0·5
Li in 3*b*	0	0	0·5	19 ± 8	0·5
O in 12*k*	0·223(4)	0·399(3)	0·747(4)	100	0·5

R Factor at convergence $= \sum I_{obs}/\sum (I_{obs} - I_{calc}) = 0{\cdot}0605$.
Number of intensities evaluated = 33.
Radiation: monochromatized CuK_α.
2Θ Range explored: 18 to 100.
Space group: $P6_222$ (No. 180).
Unit cell dimensions (nm): $a_0 = 0{\cdot}528$, $c_0 = 1{\cdot}115$.

order → disorder transition for the lithium atoms, too. Superstructure XRD reflections of the *c*-type would decrease to zero insensitivity, therefore halving c_0.

Among the different samples examined, only E1 (characterized by a stoichiometric ratio Li:Al:Si of 1:1:1) displays superstructure of the *c*-type, and therefore some degree of Si–Al ordering, in contrast to the other samples E2, E3 and E4.

In order to better clarify these points, the four monophasic compositions E1 to E4 were submitted to a measure of the diffracted X-ray peak intensities (Cu K_α radiation). The data were computer-collected (step scan interval 2Θ = 0·005, count time = 2 s) and further elaborated for background subtraction, net intensity evaluation, Lorentz and polarization correction. Overlapping peaks were deconvoluted using a Lorentzian curve fitting. The peaks used ranged from 10 to 80 degrees 2Θ. The independent coordinates and the occupation factors for the Li, Al and Si atoms were refined on the basis of the XRD net intensities using a full-matrix least-squares procedure, starting from the high-temperature β-eucryptite structure in the space group $P6_222$ (No. 180) for sample E1, and from the β-quartz structure in the same space group for the sample E2 to E4.

The results of the E1 refinement, reported in Table 2, are substantially in agreement with the results of Ref. 13 for the high-temperature phase. Apart from a slight difference in the fractional oxygen coordinates, the main discrepancy is the lithium position, that in this refinement is partially distributed between the two possible positions, namely 3*a* ($z = 0$, 1/3, 2/3) and 3*b*($z = 1/6$, 1/2, 5/6) with a relative occupancy of about 19% and 31% respectively (Fig. 1(b)). However, the uncertainty of the result is rather high, due to the low scattering power of lithium (Table 2). In Ref. 13, Li atoms were placed exclusively in the 3*a* position, although the same authors reported residual peaks in the difference Fourier syntheses, indicating that some Li is disordered on the 3*b* position too.

Al and Si atoms were refined for E1 on the two different crystallographic positions, namely 3*c* and 3*d*. The results of this refinement indicate a preferred occupation of Si and Al on 3*c* and 3*d* positions respectively, even if the scattering power of these two elements is rather similar. The reliability factor (R) increases regularly by trying a gradual reciprocal substitution of Al and Si on the above positions, from a value of 0·0605 (no substitution) to 0·0691 (reversed occupation, i.e. Al on 3*c* and Si on 3*d*). The location of Al and Si is also confirmed by the calculated mean Si–O and Al–O interatomic distances (164 and 171 pm), which agree well with the literature values. The thermal isotropic factors remained fixed to 0·5, as their refinement brings no significant improvement to the R factor.

In the β-quartz structure of the samples E2, E3 and E4, Al and Si are, in contrast, randomly distributed on a 3*c* position and oxygen is located in the 6*j* position, of the x, $2x$, 1/2 type, with $x \approx 0{\cdot}20$ for all the three samples. Li atoms occupy a position of the 3*a* type with a 50% occupancy and are therefore randomly distributed among all the possible tetrahedral voids of the channels.

The sample C1, crystallized at 900°C for 16 h showed no hints of superstructure reflections either of *a*- or *c*-type. In this case indeed the Al:Si ratio has the value of 1·25, the same as sample E2, a value which has been shown to hamper the Al–Si ordering in the E series of samples. Moreover, the Mg ions occupy only about 22% of the vacant tetrahedral interchannel positions, a fact that clearly favors disordering of these ions.

2.5 IR characterization

The IR spectra of the crystalline samples E1 to E4 and C1 are shown in Fig. 5. The spectra can be interpreted on the basis of the known IR spectra of the silica polymorphs,[15–17] including those of α(low)-quartz and of amorphous silica and silica–alumina, reported in Fig. 6. The IR spectra of SiO_2 polymorphs, constituted by tetrahedrally coordinated Si atoms, are characterized by three groups of bands: (i) a very strong complex of bands,

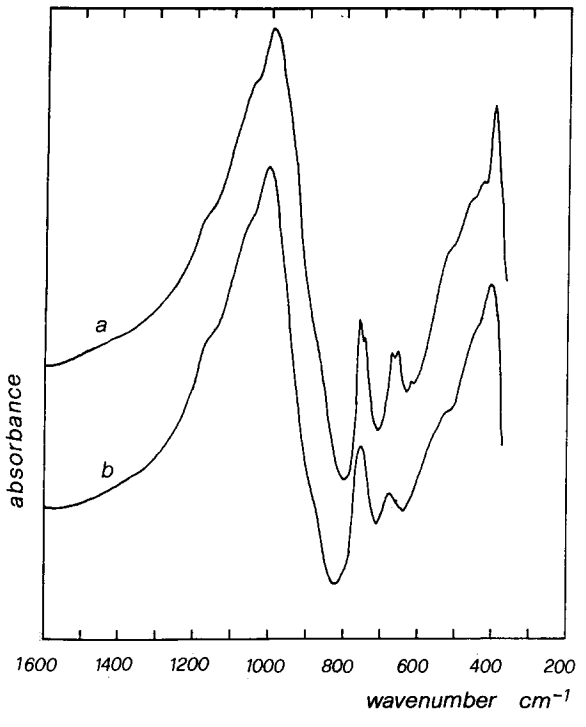

(a)

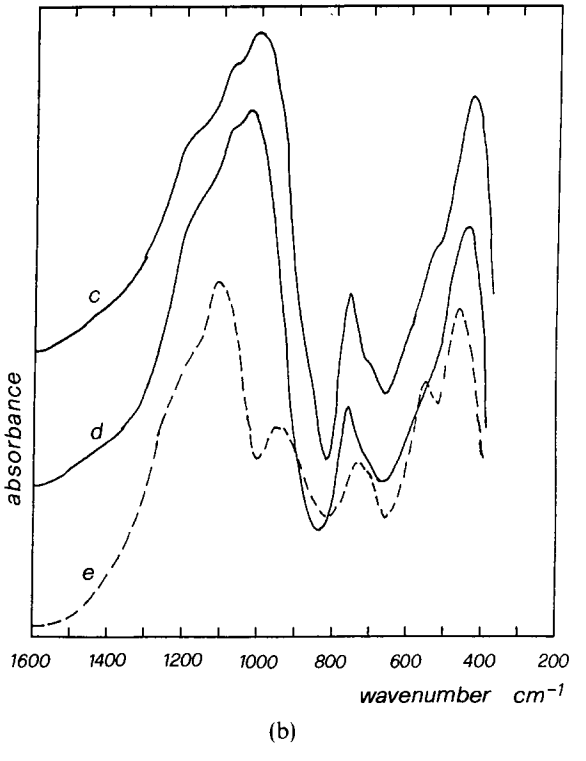

(b)

Fig. 5. FTIR spectra (KBr pressed disks) of β-quartz-type phases. (a) E1 (β-eucryptite); (b) E2; (c) E3; (d) E4; (e) C1 (μ-cordierite).

whose main maximum is invariably detected in the 1110–1090 cm^{-1} range, due to asymmetric Si–O–Si stretching modes; (ii) a medium complex of bands in the 820–650 cm^{-1} region, due to symmetric Si–O–Si stretching modes; (iii) one or more strong bands in the region 500–400 cm^{-1} assigned to deformation modes.

Unfortunately, the exact positions of the IR active bands of the β-quartz polymorph are not

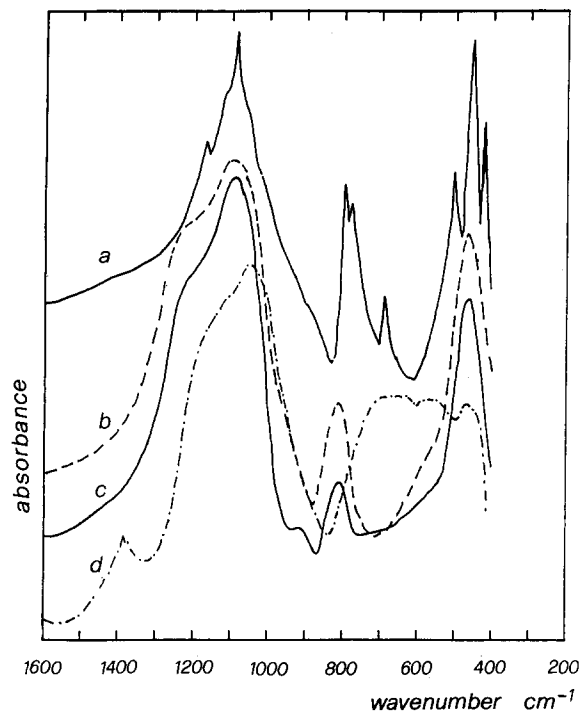

Fig. 6. FTIR spectra (KBr pressed disks) of (a) α-quartz; (b) amorphous silica (Aerosil); (c) amorphous silica–alumina (13% Al_2O_3); (d) amorphous precursor to cordierite $Mg_2Al_4Si_5O_{18}$.

known,[18,19] because of the difficulty in obtaining high-temperature IR spectra of powdered samples. High-temperature monocrystal IR reflection studies have been reported for quartz,[20,21] and show a continuous shift down of all vibrational modes upon heating α-quartz during the phase transition to β-quartz (occurring at 573°C) and the disappearance of at least one vibrational mode. This, however, is only partly in agreement with calculations based on the Raman spectra of α- and β-quartz,[18,19] because an increase of the IR active asymmetric Si–O stretching frequency is expected. The disappearance of some IR active modes is due to the increase of the symmetry of the structure during the α-to-β transition.

The spectrum of E1 only partially agrees with that reported previously for another synthetic β-eucryptite sample.[22] It is composed by sharp bands, indicating a high ion ordering in the structure. It shows the Si–O–Si asymmetric stretching modes to be very strong, with the maximum at 996 cm^{-1}, and shoulders at 1050 and 1160 cm^{-1} (Table 3). In the region of the symmetric Si–O stretching modes, two sharp doublets of medium strength are observed at 757 and 744 cm^{-1}, and 673 and 657 cm^{-1}, while the deformation mode shows the maximum at 405 cm^{-1}, with pronounced components at 432, 468 and 520 cm^{-1}.

In series $Li_xAl_xSi_{3-x}O_6$ some progressive spectral modifications are observed by decreasing x: (i) the main maximum of the Si–O–Si stretching mode shifts to higher frequencies up to near 1030 cm^{-1} and broadens; (ii) the doublet at 673 and

Table 3. IR skeletal bands (cm^{-1}) of β-quartz-type aluminosilicates

Assignment	*E1*	*E2*	*E3*	*E4*	*C1*
Si–O–Si asymmetric stretching	1160 sh 1050 sh 995 vS	1165 sh 1050 sh 1000 vS	1190 sh, br 1070 sh 1005 vS	1190 sh 1070 1030 vS, br	1242 sh 1180 sh 1108 vS
Al–O stretching	—	—	—	—	940 m, br
Si–O–Si symmetric stretching	757 744 673 657	751 m 710 sh 670 w	750 m 695 sh	750 m 689 sh	730 m 695 sh
$M^{a}O_4$ stretching	520 m, sh	530 m, sh	523 sh	560 sh	545 ms
Si–O–Si deformation	470 sh 405 vS	465 m 410 vS	505 sh 430 vS	438 S	460 S

[a] $M = Li^+$ or Mg^{++}.
sh = sharp; br = broad; vS = very strong; m = medium; ms = medium strong; s = strong.

$657\,cm^{-1}$ is strongly decreased for $x = 1{\cdot}33$ and disappears for $x = 1{\cdot}15$ and $1{\cdot}00$; (iii) the doublet at 757 and $744\,cm^{-1}$ transforms into a single, although asymmetric, band at $750\,cm^{-1}$ with a shoulder near $695\,cm^{-1}$; (iv) the main maximum of the deformation band shifts up to $438\,cm^{-1}$, while the shoulders at its higher frequency side decrease in intensity; (v) in general, the spectrum loses resolution significantly.

The progressive loss of the high spectral resolution by increasing the Si/Al ratio is likely to be related to an increasing disorder in the cation distribution, i.e. Si and Al in the framework and Li in the tetrahedral voids, according to what is observed by XRD.

The shift to lower frequencies of the position of the main maximum of the ν_{as} Si–O with increasing Al substitution for silicon in the tetrahedral silicate framework has been observed in the cases of different aluminosilicate structures.[23–26] This shift seems to be primarily due to Al for Si substitution. However, a role of the counterion on this shift has also been shown, e.g. in glasses[24] and crystalline tectosilicates of the sodalite family.[27] In the case of isostructural compounds this effect is in the sense of a stronger shift down of the ν_{as}Si–O–Si frequency by decreasing the size of the cation.[27] So, this means that the larger the countercation, the smaller the shift down of ν_{as}Si–O–Si complex of bands, for the same Al and Si substitution degree. For crystalline tectosilicates like sodalites[27] a shift upwards of the deformation mode parallels the shift down of ν_{as}Si–O, as in the present case.

These effects should be related to 'chemical factors' more than to geometric factors. It is in fact well known that the symmetric stretching modes of SiO_4 tetrahedra ($1200–800\,cm^{-1}$) fall at higher frequencies than those of AlO_4 octahedra ($1000–700\,cm^{-1}$).[28,29] An Al for Si substitution could consequently cause a shift down of the stretching mode of SiO_4–AlO_4 frameworks. The effect of the countercation (the stronger the effect the smaller the size) can be related to the value of the polarizing power of the cation. The smaller cations interact stronger with the oxygen atoms involved in the (Si,Al)–O–(Si,Al) bridges. In the present case this effect is also expected to depend on the amount both of Al^{3+} in the framework and of Li^+ in the interstices.

The analysis of the spectra in Fig. 5 shows that at the higher frequency side of the deformation mode an absorption grows with increasing x, centered near $530\,cm^{-1}$, with perhaps a second one near $470\,cm^{-1}$. Indeed, the deformation mode in silica polymorphs can split into several components. However, the spectra only show weak shoulders, if any, above $500\,cm^{-1}$. Partial substitution of Al for Si is probably not responsible for the formation of bands in the $600–500\,cm^{-1}$ region. In fact the deformation modes appear to be only slightly shifted upwards by this substitution. Consequently, the new absorption near $530\,cm^{-1}$, apparently related to cavity occupancy by Li^+, can be due to symmetric stretching modes of LiO_4 tetrahedra. These groups, in fact, have been shown to be responsible for bands in the $600–450\,cm^{-1}$ region in various compounds including, for example, the high-temperature form of $LiAlO_2$ (gamma form).[30] The growth of the shoulder at $530\,cm^{-1}$ in the series $Li_xAl_xSi_{3-x}O_6$ with increasing x can consequently be taken as evidence of the occupancy of tetrahedral interstitial sites of the β-quartz structure by Li^+ cations. The further shoulder near $470\,cm^{-1}$ in the spectrum of β-eucryptite could be due to deformation modes of Al–O–Si or Al–O–Al bridges.

The position of the more intense symmetric Si–O–Si stretching mode is apparently weakly perturbed by increasing x. This agrees with the data obtained by Al for Si substitution, e.g. for zeolites,[31] probably because their very small mass difference. However, this mode is very sensitive to the symmetry of the structure: in fact it should vanish if the (Si,Al)–O–(Si,Al) bridge angle is 180°, and can split in

more components. In particular, three bands belonging to this mode are found in the IR spectrum of powdered α-quartz (Fig. 6), according to the literature.[17] However, the symmetry of the β-quartz structure (D_6^4 or D_6^5 enantiomeric space groups) is higher than that of the α-polymorph (D_3^4 or D_3^6 enantiomeric space groups). So, one mode only belonging to the symmetric Si–O–Si stretching is expected to be active in IR for β-quartz.[18,19] This agrees with the disappearance of the band (near 700 cm^{-1}), with quartz monocrystals when the temperature is enhanced above the α-to-β transition.[20,21] This mode observed at 695 cm^{-1} in transmission spectra of powdered α-quartz (Fig. 6), has been assigned to an *E*-symmetry mode in α-quartz (both IR and Raman active) but should convert into an E_2-type mode (Raman active only) for the space group of β-quartz.

The spectra show two doublets for *E*1 ($x = 1{\cdot}5$), that become a single, although asymmetric, band for *E*4 ($x = 1$). Intermediate features are found for *E*2 ($x = 1{\cdot}33$) and *E*3 ($x = 1{\cdot}15$). The progressive disappearance of the doublet at 673 and 657 cm^{-1} in the IR spectra of $Li_xAl_xSi_{3-x}O_6$ by decreasing x from 1·5 to 1 is strongly reminiscent of the disappearance of the mode near 700 cm^{-1} during the α-to-β quartz transition, due to the increase of symmetry.

The absence of this mode in the samples E4 and E3, consequently, should confirm that the geometry of the structure of these samples is the same of β-quartz. It can be noted that the composition of the sample with *E*4 is such that one Li^+ can enter in one β-quartz-type cell, where three tetrahedral cavities are present, two of which must remain vacant.

In contrast, the appearance of the symmetric Si–O stretching mode responsible for the doublet at 673 and 657 cm^{-1} in the IR spectrum of the synthetic analogue of β-eucryptite suggests a lowering of the symmetry by approaching $x = 1{\cdot}5$. This fact can be related to the XRD evidence of a different position of the oxygen atoms: in E1 sample they occupy a generic 12-fold position of the x,y,z type (Table 2), whilst in the other E samples they are placed in a more symmetric sixfold position of the $x,2x,1/2$ type. The detection of the above doublet indicates clearly that the coordination symmetry of the oxygen atoms around the Si/Al atoms in the structure is lower. It can be noted that the spectrum previously published for β-eucryptite[22] did show a band corresponding to the doublet observed here.

The spectrum of the β-quartz form of cordierite, the so-called μ-cordierite, is also presented in Fig. 5. In spite of the structure similar to β-eucryptite, as deduced by XRD measurements, the IR spectra differ significantly from those of the $Li_xAl_xSi_{3-x}O_6$ solid solutions, as already discussed.

The spectrum shows broad structures, indicating a significant disorder in the structure. The asymmetric Si–O stretching bands are constituted by a complex of bands whose main maximum is at 1105 cm^{-1}, and presents at its low frequency site a broad but intense band at 940 cm^{-1}. The symmetric stretching mode is characterized by a weakly split band whose maximum is at 730 cm^{-1} and a second component is near 695 cm^{-1}. The deformation mode is observed at 460 cm^{-1} very strongly, but another band is found at its high frequency side, at 545 cm^{-1}. The spectrum, although similar, does not completely agree with that presented recently for a similar preparation,[32] and differs significantly also from that discussed by Langer & Schreyer several years ago.[33]

The characteristic band found at 940 cm^{-1}, quoted by Merle-Mejan *et al.*[32] at 960 cm^{-1} and by Langer & Schreyer at 950 cm^{-1} (but in the spectrum presented by these authors[33] it appears to be far more intense than in the present case), is not present in the spectra of silica polymorphs. A band in this region is generally not found in the spectra of tectosilicates, but can be present in those of other silicates, and is assigned to the terminal Si–O bond. For this reason, strong bands in this region are found in the spectra of the cyclosilicates α- and β-cordierite.[32–34] However, these modes are not expected in β-quartz-type structures, because of the absence of terminal Si–O bonds. Bands in this region have also been assigned to modes of Si–OH bonds in hydrated glasses,[35] phyllosilicates,[23] etc. However, these modes are also not expected in the present material.

Interestingly, the component at 940 cm^{-1} is present neither in the spectrum of the amorphous material precursor for the μ-cordierite (Fig. 6(d)), nor in that of the amorphous precursor reported by Merle-Mejan *et al.*[32] In the spectra of these amorphous materials a broad absorption extends from 700 to 400 cm^{-1}, unusual in aluminosilicates. In contrast, the band near 950 cm^{-1} is present in the spectrum of the glass precursor reported by Langer & Schreyer,[33] showing that the starting material of this study is different, as it is also probably the resulting μ-cordierite. Indeed, a band here has been reported for Mg–Si–Al glasses having compositions similar to that of the present case.[25]

Another possible assignment for this mode is to the vibration of AlO_4 tetrahedra.[28] In fact, a number of compounds involving AlO_4 tetrahedra absorbs in this region. A band near 950 cm^{-1}, although weak, can also be found in the spectra of amorphous silica–alumina (Fig. 6(c)), where Al is thought to enter into the tetrahedral amorphous silica framework,[36] while it is absent in the spectrum of amorphous silica (Fig. 6(b)). The formation of this band upon crystallization is reminiscent of the previous study concerning the crystallization of

amorphous alumina.[37] In the amorphous state Al takes octahedral coordination, and bands are not present in the region 1000–700 cm^{-1}, while upon crystallization in the defective spinel-type structure, where AlO_4 tetrahedra are present, absorption grows strongly in this region. The modification of the spectrum upon crystallization of μ-cordierite from the amorphous precursor can be due to the change in coordination of Al from octahedral, responsible for strong absorption in the region 600–500 cm^{-1}, to tetrahedral, responsible for the band near 940 cm^{-1}.

The difference in the region 1200–900 cm^{-1} of the spectra of the sample *E*2 and of μ-cordierite *C*1, that have the same Si-to-Al ratio, can be related to the difference in number and charge of the countercations. In the Li compound the more intense asymmetric stretching mode of the tetrahedra framework is found near 1000 cm^{-1} (although the existence of a masked component near 950 cm^{-1} cannot be completely excluded), while in the Mg compound this mode is clearly split into two components, one at 1105 cm^{-1}, having the character of a Si–O–Si asymmetric stretching, and a second at 940 cm^{-1}, having the character of a symmetric stretching of AlO_4 tetrahedra. The 'separation' of these modes can be related most probably to the interaction of some tetrahedra with external Mg^{2+} cations, whose polarizing power is stronger than that of Li^+ ions, than to a non-statistical distribution of Si and Al in the β-quartz framework.

The bands at 730 and 690 cm^{-1} are certainly due to the symmetric stretching mode of the tetrahedra framework, although its position, shifted to lower frequencies than in the case of silica polymorphs, is indicative of the perturbation of (Si, Al)–O–(Si, Al) bridges by Mg cations. The strong band at 460 cm^{-1} is assigned to the deformation mode of the β-quartz-type framework, poorly perturbed. Instead, the rather strong band at 545 cm^{-1} is not common to silica polymorphs and can reasonably be assigned to vibrations involving the coordination sphere around Mg^{2+}. If this assignment is correct, it is indicative of a nearly tetrahedral coordination of Mg^{2+},[38] according to the expected location of countercations in the β-quartz.

3 Conclusions

3.1 Amorphous xerogels

The preparation route employed here furnish high homogeneity in the cation distribution. Noticeable are the surface characteristics, particularly for the C1 (μ-cordierite) composition, which displays very high areas (800 to 900 m^2/g) and peculiar pore-size distribution, that substantially persists up to about 800°C. IR evidence suggests that the amorphous precursor contains octahedral aluminium, possibly in the form of amorphous alumina of Mg aluminate rafts.

3.2 Crystallized products

The IR spectrum and XRD data of the E1 sample ($LiAlSiO_4$) furnish evidence for an ordered Si/Al framework, suggesting that the coordinative symmetry for Si and Al should be lower than that of β-quartz. This is probably related to the location of oxygen in a position of lower symmetry (12*k* space group $P6_222$ No. 180), in respect to β-quartz (6*j* space group $P6_222$). Moreover Li atoms distribute in the tetrahedral voids along *z* differently on 3*a* and 3*b* positions. The spectra of the $Li_xAl_xSi_{3-x}O_6$ solid solutions ($x > 1{\cdot}5$) indicate in contrast an increasing disorder in the Li and Al/Si locations, and a consequent increase of the average symmetry of the structure.

As regards the μ-cordierite phase, the IR and XRD results show a strong disorder in cation distribution. In the present material the octahedral aluminium in the amorphous precursor converts into tetrahedral upon crystallization to the μ-cordierite phase. The IR spectra also support the location of Mg^{2+} in tetrahedral interstices of the β-quartz structure.

References

1. Buerger, M. J., Stuffed derivatives of silica structures. *Amer. Mineral.*, **39** (1954) 600–14.
2. Roy, R., Silica O, a new common form of silica. *Z. Kristallogr.*, **111** (1959) 185–9.
3. Scheidler, H. & Rodek, E., Li_2O–Al_2O_3–SiO_2 glass–ceramics. *Ceram. Bull.*, **68** (1989) 1926–30.
4. Winkler, M. J., Crystals based on the silica structure. *Amer. Mineral.*, **33** (1948) 751–2.
5. Nakagawa, K. & Izumitani, T., Metastable phase separation and crystallization of Li_2O–Al_2O_3–SiO_2 glasses: determination of miscibility gap from the lattice parameters of precipitated β-quartz solid solution. *J. Non-Cryst. Sol.*, **7** (1972) 168–80.
6. Satyabrata, R. & Muchow, G. M., High-quartz solid solution phases from thermally crystallized glasses of compositions (Li_2O,MgO).Al_2O_3.nSiO_2. *J. Am. Ceram. Soc.*, **51** (1968) 678–82.
7. Anon., *Phase Diagrams for Ceramicists*. American Ceramic Society, 1964, p. 167.
8. Schreyer, W. & Schairer, J. F., Metastable solid solutions with quartz-type structures on the join SiO_2–$MgAl_2O_4$. *Z. Kristallogr.*, **116** (1961) 60–82.
9. Suzuki, H., Saito, H. & Hayashi, T., Thermal and electrical properties of alkoxy-derived cordierite ceramics. *J. Eur. Ceram. Soc.*, **9** (1992) 365–71.
10. Okuyama, M., Fukui, T. & Sakurai, C., Effects of complex precursors on alkoxide-derived cordierite powder. *J. Amer. Ceram. Soc.*, **75** (1992) 153–60.
11. Bansal, N. P., Influence of several metal ions on the gelation activation energy of silicon tetraethoxide. *J. Amer. Ceram. Soc.*, **73** (1990) 2647–52.
12. Lowell, S. & Shields, J. E., *Powder Surface Area and Porosity*. Chapman and Hall, 1984, p. 54.
13. Pillars, W. & Peacor, D., The crystal structure of beta-eucryptite as a function of temperature. *Amer. Mineral.*, **58** (1973) 681–90.

14. Tscherry, V. & Leaves, F., Synthesis and X-ray reflection pattern of β-eucryptite. *Naturwissenschaften*, **57** (1970) 194.
15. Gadsden, J. A., *Infrared Spectra of Minerals and Related Inorganic Compounds*. Butterworths, 1975.
16. Griffith, W. P., In *Spectroscopy of Inorganic-based Materials*, ed. R. J. H. Clark & R. E. Hester. Wiley, 1987.
17. Bliss, M., Walden, B. L. & White, W. B., Measurement of infrared spectra of dense ceramics by specular reflectance spectroscopy. *J. Amer. Ceram. Soc.*, **73** (1990) 1078–83.
18. Etchepare, J., Merian, M. & Smetankine, L., *J. Chem. Phys.*, **60** (1974) 1873.
19. de Vos Burchart, E., van Bekkum, H. & van de Graaf, B., Molecular mechanics study on the α-quartz/β-quartz transition. *J. Chem. Soc., Faraday Trans.*, **88** (1992) 1161–4.
20. Simon, I. & McMahon, H. O., *J. Chem. Phys.*, **21** (1953) 23.
21. Gaskell, P. H., *Trans. Faraday Soc.*, **62** (1966) 1493–504.
22. Murthy, M. K. & Kirby, E. M., *J. Amer. Ceram. Soc.*, **45** (1962) 324–9.
23. Farmer, V. C. & Russel, J. D., The infrared spectra of layer silicates. *Spectrochim. Acta*, **20** (1964) 1149–73.
24. Lyon, R. J. P. & Tuddenham, W. M., *Nature*, **185** (1960) 374.
25. Roy, B. N., Infrared spectroscopy of lead and alkaline-earth aluminosilicate glasses. *J. Amer. Ceram. Soc.*, **73** (1990) 846–55.
26. Flanigen, E. M., Khatami, H. & Szymanski, H. A., *Adv. Chem. Ser.*, **101** (1971) 201.
27. Henderson, C. M. B. & Taylor, D., Infrared spectra of anhydrous members of the sodalite family. *Spectrochim. Acta*, **33A** (1977) 283–90.
28. Tarte, P., Infrared spectra of inorganic aluminates and characteristic vibrational frequencies of AlO_4 tetrahedra and AlO_6 octahedra. *Spectrochim. Acta.*, **23A** (1967) 2127.
29. Moolenaar, R. J., Evans, J. C. & McKeever, L. D., *J. Phys. Chem.*, **74** (1970) 3629.
30. Tarte, P. & Preudhomme, J., ^6Li–^7Li shifts in the infrared spectrum of inorganic lithium compounds. II. Rhombohedral $LiXO_2$ compounds. *Spectrochim. Acta*, **26A** (1969) 747–54.
31. Szostak, R. & Thomas, T. L., Reassessment of zeolite and molecular sieve framework infrared vibrations. *J. Catal.*, **101** (1986) 549–52.
32. Merle-Mejan, T., Vesteghem, H., Quintard, P. & Lorenzelli, V., FT–IR investigation of cordierite aerogel. *J. Mol. Struct.*, **175** (1988) 401–6.
33. Langer, K. & Schreyer, W., Infrared and powder X-ray diffraction studies on the polymorphism of cordierite $Mg_2(Al_4Si_5O_{18})$. *Amer. Mineral.*, **54** (1969) 1442–59.
34. Ismail, M. G. M. U., Tsunatori, H. & Nakai, Z., Preparation of mullite cordierite composite powders by the sol–gel method: its characteristics and sintering. *J. Amer. Ceram. Soc.*, **73** (1990) 537–43.
35. Uchino, T., Sakka, T. & Iwasaki, M., Interpretation of hydrated states of sodium silicate glasses by infrared and Raman analysis. *J. Amer. Chem. Soc.*, **74** (1991) 306–13.
36. Léonard, A., Suzuki, S., Fripiat, J. J. & DeKimpe, C., *J. Phys. Chem.*, **68** (1964) 2606.
37. Abbattista, F., Delmastro, A., Gozzelino, G., Mazza, D., Vallino, M., Busca, G. & Lorenzelli, V., Effect of phosphate ions on the surface chemistry and microstructure of amorphous alumina. *J. Chem. Soc., Faraday Trans.*, **86** (1990) 3653.
38. Gabelica-Robert, M. & Tarte, P., Vibrational spectrum of akermanite-like silicates and germanates. *Spectrochim. Acta*, **35A** (1979) 649–54.